Generation of 10m Resolution PalSAR and JERS-SAR Mosaics and Forest/Non-Forest Maps For Forest Carbon Monitoring

M. Shimada[1)], O. Isoguchi[1)], T. Motooka[1)], T. Shiraishi[1)], A. Mukaida[2)], H. Okumura[2)], T. Otaki[2)], T. Itoh[2)], A. Rosenqvist[3)], A Kato[4)], and T. Sasai[4)]

[1)] Earth Observation Research Center, Japan Aerospace Exploration Agency, Sengen2-1-1, Tsukuba, Ibaraki, 305-8505, Japan

[2)] Remote Sensing Technology Center of Japan

[3)] Solo Earth Observation (soloEO)

4) Division of Earth and Environmental Sciences Graduate School of Environmental Studies, Nagoya University

E-mail: shimada.masanobu@jaxa.jp

Abstract - The Japan Aerospace Exploration Agency (JAXA) has produced the world's first 10m resolution L-band SAR global mosaic datasets. These data sets were generated to monitor forest changes from the 1990s to present time. SRTM-3 (90m resolution) DEM was used for correct for terrain-induced SAR image variations and for ortho-rectification. Both corrections were applied for geometric and radiometric calibration purposes. The data sets are useful for monitoring forest cover and forest change, and were used to derive forest/non-forest information.

I. INTRODUCTION

Reducing of Emission from Deforestation and forest Degradation plus (REDD+) is an international collaborative work to decrease forest carbon emissions from developing countries with the aim to suppress global warming. In order to enable monitoring of forest carbon and emissions, several countries are in the process of establishing national MRV (Measurement, Reporting and Verification) systems for their forests. This requires long time-series of high-resolution spaceborne sensor data and ground truth data. In order to successfully monitor the forests from spaceborne sensors, several requirements are given, i.e., 1) high resolution imaging of more than 25m, 2) high frequency observation (1/year or better), and 3) measurement of forest geophysical parameters (i.e., forest/non-forest, and biomass) [1]. Landsat provides the longest time-series observation capability after the 1970s, and SPOT is the second longest. While their weak point is the cloud coverage, Synthetic Aperture Radar (SAR) is all-weather sensor that is unaffected by clouds and haze. JAXA has for a long time been acquiring L-band SAR data over the global land areas – between 1992 and 1998 by the Japanese Earth Resources Satellite-1 (JERS-1) SAR and since 2006 by using ALOS PALSAR. Among spaceborne SAR systems, L-band SAR is the most advantageous for detecting forest information (i.e. biomass, deforestation area, and its change rate) because lower radio frequency (longer wavelength) signals are more sensitive to forest structure (smaller ratio of surface roughness to the wavelength at the lower frequency increases the contrast of forest/non-forest) and the higher signal penetration through the forest canopy allows the detection of the biomass of the trunks.

2. NECESSITY CONDITIONS FOR GLOBAL FOREST MONITORING USING SAR

In order to assure that the satellite sensor and SAR data can be utilized for global forest monitoring, they need to meet the following conditions:

1) The sensor has to be well stabilized.
2) Accurate radiometric and geometric calibration
3) Accurate ortho-rectification
4) Accurate slope correction
5) Accurate mosaicking
6) Forest/non-forest and land classifications

The JERS-1 SAR and ALOS PALSAR both satisfy conditions 1)~5) [2-4]. Condition 6) is met through the use of the Support Vector Machine algorithm [5]. Here, we show some key conditions met for the PALSAR data below. We show the two issues, i.e., slope-correction for the PALSAR data and geometric accuracy of the ortho-rectification.

3. SLOPE-CORRECTION OF THE PALSAR IMAGE

Slope correction of the SAR image is a process to suppress or eliminate the terrain induced intensity variation of the SAR image. The following two equations summarize the conversion from the sigma-naught to gamma-naught.

The slope corrected $\gamma^0$is often used for forest data analysis because the diffuse reflection rather reduces the incidence angle dependency [13]. Thus, the slope-corrected $\gamma^0$and σ^0can be converted by the following equation.

$$\gamma^0 \equiv \frac{\sigma^0}{\cos\theta_{local}} \frac{\cos\psi}{\sin\theta_{inci}} \quad (1)$$

$$\cos\psi = \mathbf{n}_f \cdot \mathbf{n}_l \quad (2)$$

Here, γ^0 is the gamma-naught, σ^0 is the sigma-naught, θ_{local} is the local incidence angle, θ_{inci} is the global incidence angle which is defined on the GRS80, and ψ an angle between the local normal vector ($\mathbf{n}_f$) and the normal vector ($\mathbf{n}_l$) perpendicular to the radar line of sight (LOS) within a plane in LOS and Center of the Earth (COE)

An example of the slope correction is shown in the following figures. Figure 1a is the slant range PALSAR image including Mt. Fuji and vicinity area, where height variation ranges from 0 m over the ocean to the 3776 m at the peak of Mt. Fuji. Figure 1b is the corresponding image after the slope correction. Here, the 50 m spaced digital elevation model of GSI (Geophysical Survey of Institute, Japan) was used.

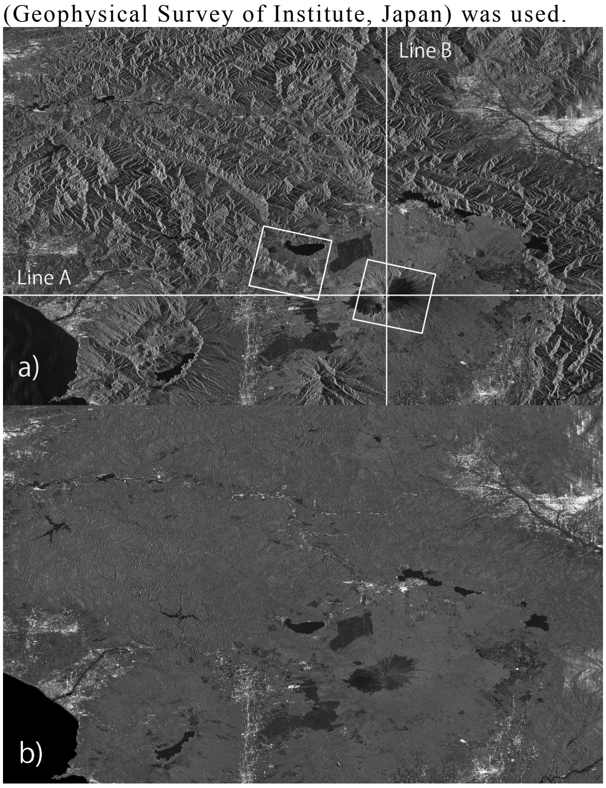

Figure 1. ALOS PALSAR images of Mt. Fuji before a) and after b) slope correction (for layover and cross section area).

4. GEOMETRIC ACCURACY OF THE ORTHO-RECTIFIED PALSAR IMAGES

Geometric accuracy of the ortho-rectification was also evaluated. Figures 2 show that the ortho-rectification was successfully conducted and the active radar calibrators in ascending and descending orbit are well matched with the theoretical cross point given from the orbital information. Geometric evaluation accuracy of these ARC (Active Radar Calibrator) positions is shown in TABLE I. This means that the geometric accuracy is quite accurate and within the order of less than 5m as the one-sigma.

TABLE I Ortho-rectified Geometric Accuracy

ARC	Δx (m)	Δy (m)	Δs (m)
Ascending	0.253	3.092	3.102
Descending	3.040	3.711	4.797

TABLE II Allocation of the data acquisitions for mosaic2009

Year	No. of strips	Ratio (%)
2007	17	1
2008	177	12
2009	1216	79
2010	122	8
Total	1532	100

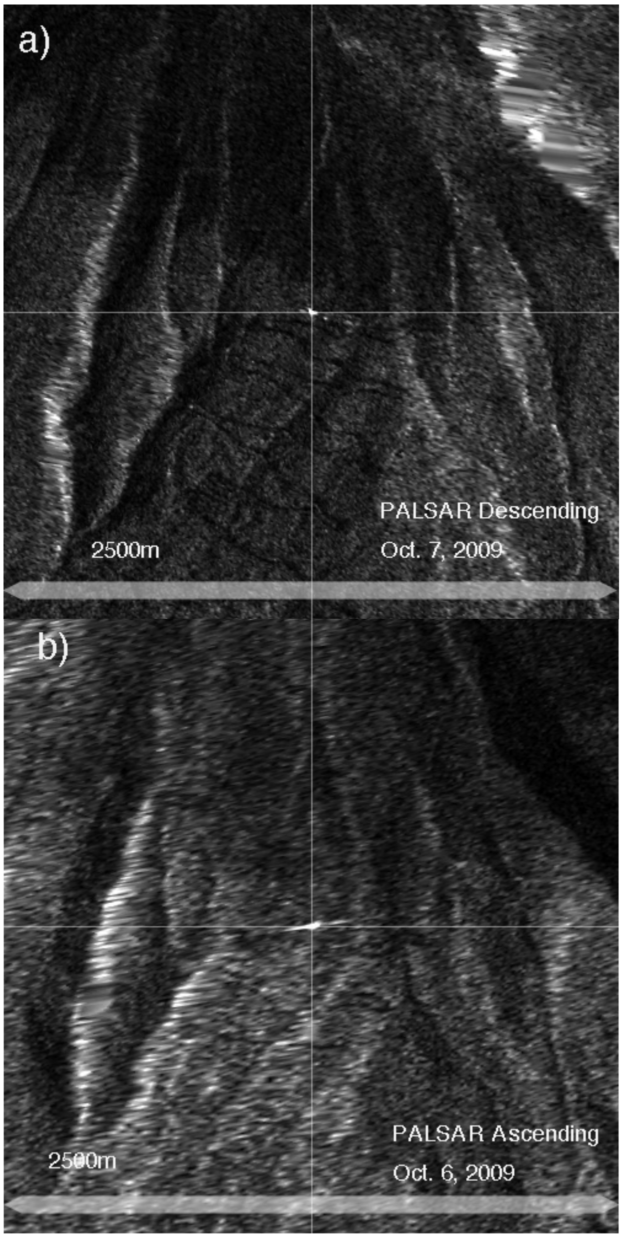

Figure 2. Two examples of geolocation evaluations are shown in a) for Mt. Fuji in a descending path and b) for Mt. Fuji in an ascending path. The two cross points of the vertical and horizontal lines show the point calculated from the ground truth data while the bright point shows the real ARC.

5. GENERATION OF THE GLOBAL SAR MOSAIC

Using these developed methods, we have generated the world's first 10m-resolution global PALSAR mosaic and forest/non-forest map [6] in Oct 2010. These datasets constitute the base for our forest monitoring system and the first step to support the building of MRV systems.

In addition to the above, 10m resolution global mosaics from 1995 (JERS-1), 2007 and 2009 (PALSAR) have been generated. These mosaics are geometrically calibrated with 10m accuracy by the use of corner reflectors. Figure 3 shows the 10m resolution PALSAR global mosaic dataset of year 2009, where 2look PALSAR data were originally generated from the raw data using the strip processing, and slope corrected, ortho-rectified using the SRTM-90m resolution global DEM, then mosaicked over the equal-latitude-longitude coordinate. Color assignment of images is HH for red, HV for green, and HH/HV for blue. Here, the green color represents the forest region and dark purple area shows the non-forest regions qualitatively.

Although the PALSAR data acquisition capability is large enough, consistent data acquisition within 92 days for one global coverage is difficult. In this case, the data allocation at each year is described in the Table II. Mosaic 2009 was produced using 1532 strips in total and 1216 (79%) are selected from 2009 year.

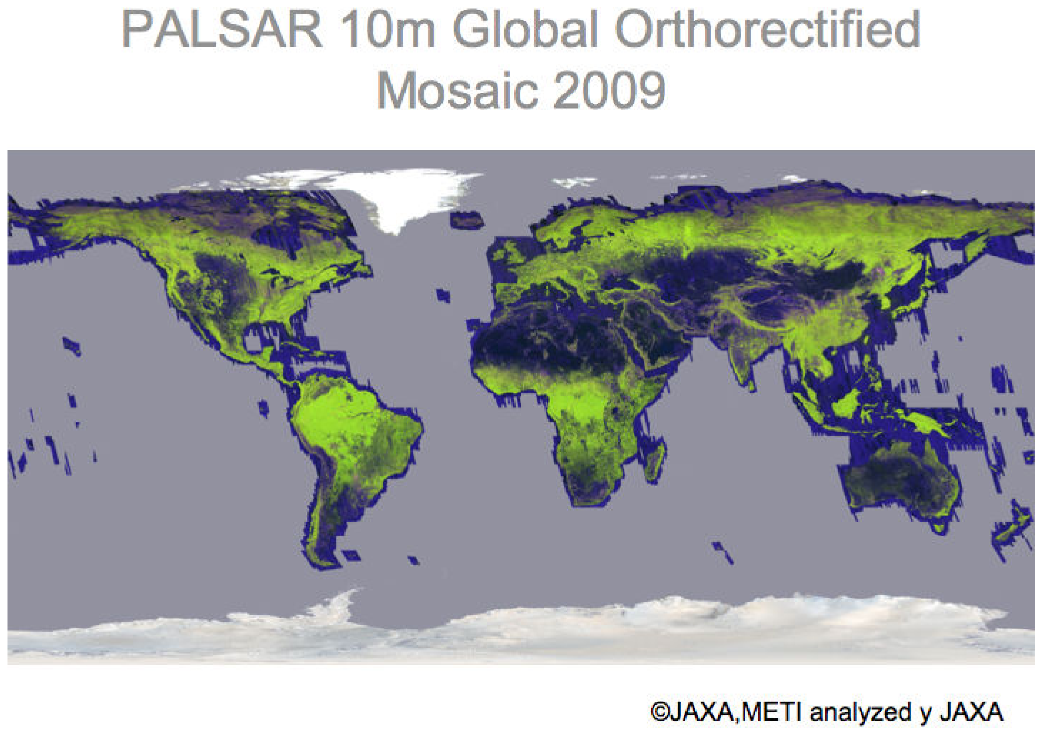

Figure 3. 10m-resolution PALSAR of 2009 acquisition

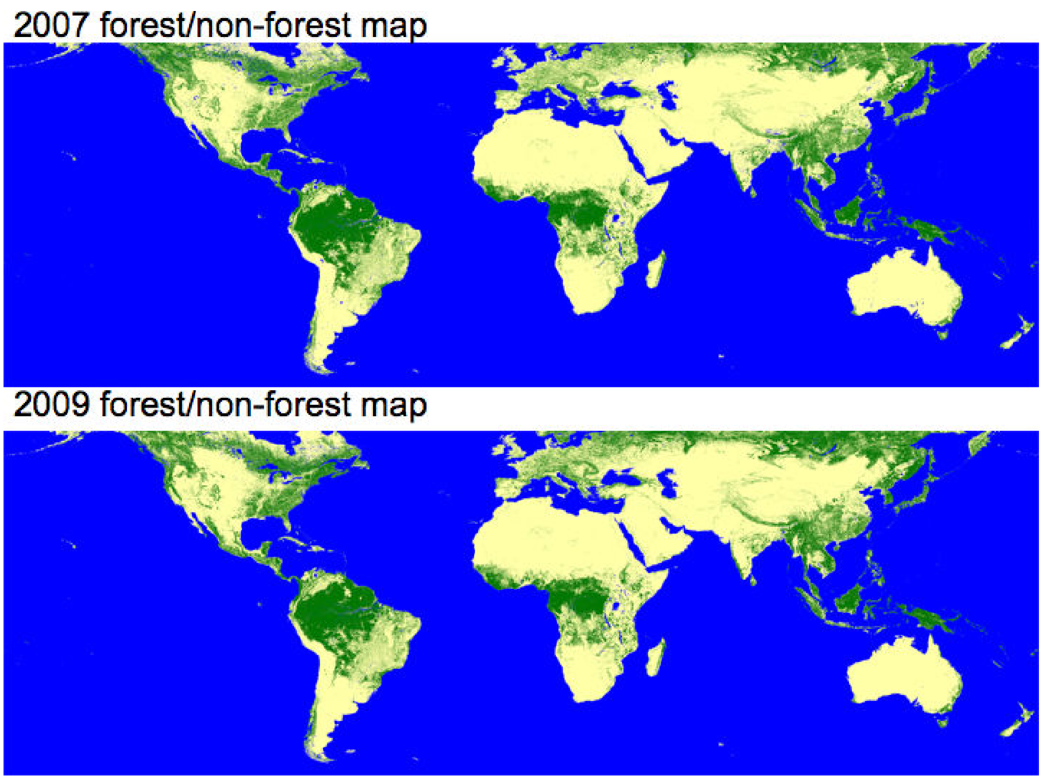

Figure 4. Forest/Non-forest map for 2007 (top) and 2009 (bottom).

6. GENERATION OF FOREST/NONFOREST

In an effort to generate a first draft forest/non-forest classification, point 6) above was undertaken with the following simplified procedure based on HV backscatter only: image segmentation, followed by a classification where forest is designated as σ^0_{hv}>-14dB~-15dB, water is σ^0_{hh}<-22dB~-20dB, while remaining areas are assigned as non-forest. Finally, a grouping process was undertaken. Figures 3 and 4 show forest/non-forest dataset for 2007 and 2009. The validation has been conducted as the direct comparison between these products and the ground truth data, which were collected from the DCP, Degree Confluence Project, at the integer latitude and longitude corners [7]. The total accuracy of agreement (Forest and non-forest) is 84% in average.

Using the method, we will be able to interpret the change of the forest as its time series. Figure 5 shows the time series of forest/non-forest at Rio Branco of Brazil. Deforestation is in progress. Figure 6 also shows the 13 years change of the forest.

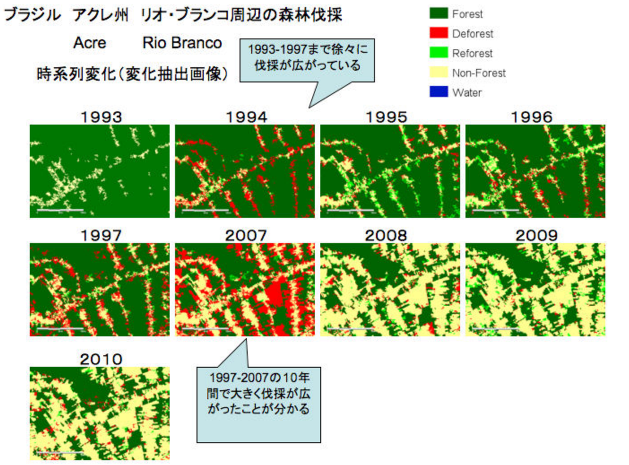

Figure 5. 17 years change of forest cover at Rio Branco, Brazil, derived from JERS-1 and ALOS PALSAR.

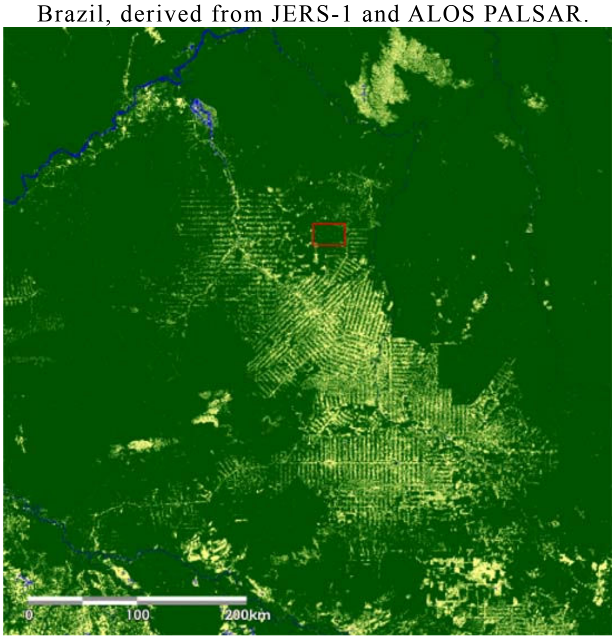

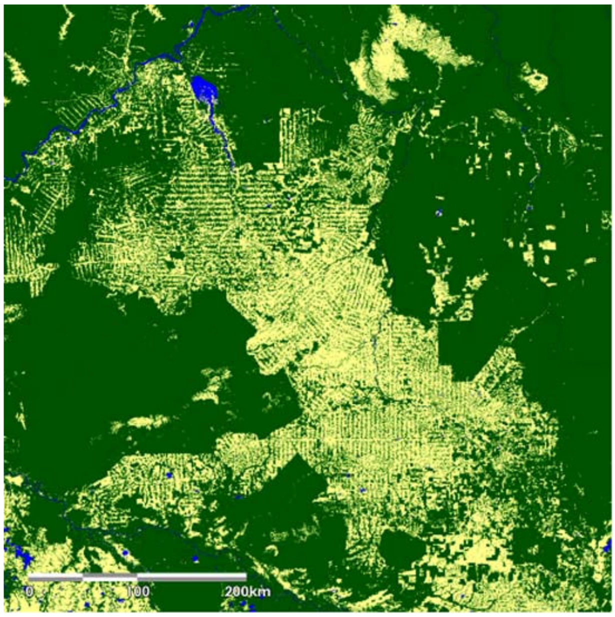

Figure 6. 13 years forest cover change in Rondonia, Brazil, using the JERS-1 SAR and PALSAR global mosaics and forest/non-forest classifications.

7. CONCLUSIONS

We have generated global-scale 10m resolution mosaic data sets using JERS-1, ALOS PALSAR and SRTM DSM. The ortho-rectified and slope corrected data can be used for the classification of the tropical rainforest. In addition to this, JAXA is going to generate the 10m-spaced global data set and forest/non-forest classification mapping.

REFERENCES

[1] GOFC-GOLD, "SOURCEBOOK COP 16 version 1".

[2] M. Shimada, O. Isoguchi, T. Tadono, and K. Isono, "PALSAR Radiometric and Geometric Calibration," IEEE Trans. GRS, VOL. 47, NO. 12, Dec. 2009, pp.3915-3932.

[3] M. Shimada and T. Otaki, "Generating Continent-scale High-quality SAR Mosaic Datasets: Application to PALSAR Data for Global Monitoring," IEEE JSTAR special issue on Kyoto and Carbon Initiative, vol. 3, Issue 4, 2010, pp. 637-656.

[4] M. Shimada, "Ortho-rectification and Slope Correction of SAR Data Using DEM and Its Accuracy Evaluation," IEEE JSTAR special issue on Kyoto and Carbon Initiative, vol. 3, Issue 4, 2010, pp. 657-671.

[5] Longépé N., Rakwatin P., Isoguchi O., Shimada M., Uryu Y., Yulianto K., "Assessment of ALOSPALSAR 50m Orthorectified FBD Data for Regional Land Cover Classification by Support Vector Machines", IEEE Transactions Geosciences and Remote Sensing, in press.

[6] JAXA/EORC web: http://www.eorc.jaxa.jp/ALOS/en/guide/forestmap_oct2010.htm

[7] DCP：http://confluence.org/